Determination of structural alloy equilibrium properties from quantum approximate methods

Jorge E. Garcés[1] and Guillermo Bozzolo[2,3]
[1]*Centro Atomico Bariloche, 8400 Bariloche, Argentina*
[2]*Ohio Aerospace Institute, Cleveland, Ohio 44142, USA*
[3]*NASA Glenn Research Center, Cleveland, Ohio 44135, USA*
(Received 25 August 2004; revised manuscript received 24 November 2004; published 11 April 2005)

In this paper we address basic issues, not investigated previously, concerning the relationship between *ab initio* methods and the Bozzolo-Ferrante-Smith (BFS) method for alloys, and its ability to model the process of alloy formation and reproduce structural alloy properties near and at equilibrium. Based on perturbation theory, the method requires single element parameters and their binary combinations, even for multicomponent systems. A direct comparison of BFS predictions of equilibrium alloy properties against *ab initio* results, and the handling and influence of the parameterization on the accuracy with which the method reproduces the process of alloy formation are presented. Besides establishing a range of validity for the method in reference to first-principles results, a simple algorithm for the determination of equilibrium properties of ordered alloy systems is introduced and illustrated with applications to binary and higher order systems, maximizing the flow of information carried in the first-principles-based parameters.

DOI: 10.1103/PhysRevB.71.134201 PACS number(s): 61.66.Dk, 71.15.−m, 71.20.Be, 61.82.Bg

I. INTRODUCTION

The vast number of potentially useful but still undiscovered alloys and the practical limitations facing the development of new materials have been the driving force for using *ab initio* methods and quantum approximate methods (qam) for large scale atomistic simulations as a standard tool to aid the experimental work on alloy design. With time, the differences (as well as the similarities) between qams and *ab initio* methods are better understood. This understanding and its consequences are now part of an overall approach to deal with the complexities of inserting computational materials design in mainstream materials development programs.

The *ab initio* approach is based in finding the solution of Schrödinger's equation which will contain all the information on the properties of the system. It is well known, however, that such solution only exists for very simple systems. This limitation has been circumvented with the use of two different approaches: one, dealing with the search of alternative, simplified, solutions which hopefully reproduce the main features of the (unknown) exact, true, solution. This is, in essence, the strategy followed by the Hartree-Fock (HF) method. A second approach, as implemented in density functional theory (DFT), consists of replacing Schrödinger's equation with one that is easier to solve, once again assuming that it is selected in such a way that its solutions are a good representation of the exact answer. In either case, in spite of these simplifications, the corresponding equations are still hard to solve, requiring a great deal of computer power and fast and efficient algorithms. Substantial progress has been realized in recent years, allowing for proper computational treatment of realistic problems.[1]

Both approaches have one thing in common: either by limiting the search of possible solutions (as in HF), or by altering the equation that properly describes the system (as in DFT), no adjustable parameters appear in these methods. In other words, simplifications are introduced without any particular reference to the system under study. Underlying this potential limitation is the fact that when implementing the simplifications that characterize either approach, the real system is replaced by a virtual one, and it is assumed that the essential features of the real system are faithfully captured.[1] The payoff warrants making these necessary changes, as complex systems can be systematically described by known and manageable algorithms with a proven record of accuracy. In essence, qams follow the same path: substantial simplifications are made for the sake of simplicity, basically opting for replacing the real system or the real process by a virtual one, but one that allows for proper tuning and optimized performance within their limited framework by means of a number, hopefully minimal, of adjustable parameters.

A recent addition to the growing family of qams is the Bozzolo-Ferrante-Smith (BFS) method for alloys,[2–5] which has been applied to a number of diverse structural problems. The method relies on approximations, by replacing the exact process of alloy formation, with virtual processes whose end result is, or is expected to be, a good description of the result of the real process. In terms of validation, the same way that DFT requires that the virtual system describe the real electron density with a high level of accuracy, BFS is expected to reproduce the essential features of the equation of state of the solid at zero temperature and, in particular, around equilibrium. Unlike *ab initio* methods that provide a full description of the system at hand (including band structure, density of states, charge density, etc.), BFS is limited to structural information that is, ultimately, contained in the binding energy curve describing the solid under study. This trade-off, i.e., greatly increased computational efficiency and a minimum number of universal parameters at the expense of detailed electronic structure information, allows for a full description of several structural aspects of interest. Starting from separate single elements as the initial state, BFS tries to provide an alternative, virtual path leading to the real final state with a minimum number of parameters to guide its way. While more flexibility can be gained by letting these parameters vary according to the specific problem at hand, no such de-

gree of freedom is added to the method, and the parameters remain fixed, fully transferable, for any case dealing with the same elements, regardless of their number, type, or structural properties. This restriction implies that in order for the method to be equally valid in a number of diverse situations, as DFT is, the parameters must contain all the necessary information to warrant the accuracy of the virtual path chosen for describing the process of alloy formation. If this description is correct, then the method should accurately reproduce the most critical properties of the solid in its final state, including the cohesive energy per atom, compressibility, and equilibrium Wigner-Seitz radius. As long as these properties are sufficient for an equally accurate description of defects, their accuracy is essential for addressing issues such as the site preference behavior of alloying additions in multicomponent systems.[3]

Approximations imply loss of information, but while to some extent such loss is affordable, it must be guaranteed that qams properly describe the properties of the final state, regardless of the path taken to model the process. Besides an ability to properly model the alloy formation process, the parameterization scheme (number of parameters, source for their determination, the information they contain, etc.) influences the accuracy with which such process is described. The BFS method relies on a minimum amount of input, namely, equilibrium properties of the pure elements (cohesive energy, lattice parameter, and bulk modulus) and their binary combinations (equilibrium lattice parameter and energy of formation of a given ordered phase).[2] In some cases, such input exists from experimental results. In order to maximize the range of application of the method, however, recent work[3–5] has centered solely on the use of input generated via first-principles (FP) methods.[6] While economical in the necessary input, the small number of parameters used in BFS imposes important demands on their stability and accuracy. Therefore, conservation of the information transferred via FP parameters is an essential requirement for the effectiveness of the method. It is also worth noting that this type of parameterization implies a somewhat different approach for the interaction between different atoms. In general, most approaches introduce some sort of interaction potential, with the parameters describing each constituent remaining unchanged. In BFS, it is precisely the set of parameters describing the pure element that it is perturbed in order to account for the distortion introduced by the nearby presence of a different element or defect. The additive nature of the perturbative theory results in that only binaries systems need to be known in the BFS framework. Multicomponent systems are thus studied only via binary perturbations.[2]

In this paper we address two basic issues concerning the method and its relationship to FP methods, namely, validation of BFS predictions of equilibrium alloy properties against FP results, and the handling and influence of the FP-based parameterization on the accuracy with which BFS reproduces the process of alloy formation. In doing so, this study focuses on the ability of the method to maximize the information from a minimum number of parameters, by examining the accuracy of predicted properties against both *ab initio* and experimental results. Section II briefly describes the full-potential linearized augmented plane wave (FLAPW) method[7] used both for the calculation of the necessary BFS parameters and for the comparison between BFS and FP results. Section III concentrates on the BFS formalism as an introduction to Sec. IV, where its relationship with FP calculations is addressed. Section V concludes with the description of an algorithm linking the BFS method and FP calculations, capitalizing on the underlying simplicity of the universal binding energy relationship (UBER)[8] for optimizing the transfer of information between the original input and the calculation of alloy equilibrium properties. Conclusions are drawn in Sec. VI.

II. FIRST-PRINCIPLES CALCULATIONS

All calculations in this paper were performed using the self-consistent FLAPW method within the generalized gradient correction of Perdew *et al.*,[9] as implemented in the WIEN97 program package.[7] FLAPW is considered as one of the most accurate band structure methods currently available to solve the Kohn-Sham equation of DFT. As such, it constitutes an useful tool for checking the validity of qams when experimental data are not available.

For all single element and binary phases, local orbitals[10] were added to the FLAPW basis to describe the semicore states *3s* and *3p* of the *3d* transition metals and the *2p* state for Al. Spin-polarized contributions to the total energy were not included in our calculations. The plane wave cutoff $R_{\mathrm{mt}}K_{\mathrm{max}}$ was set to 9.0, where K_{max} is the reciprocal lattice vector cutoff, and R_{mt}, the muffin-tin sphere radius, was set to 0.9525 Å (1.8 a.u.) for all elements. The largest value of G included in the charge Fourier expansion was set to 22. We used 10 000 k points in the full Brillouin zone for all single elements in the bcc and fcc structures and 5000 k points for multicomponent systems. All total energy calculations were converged in energy to within 0.01 mRy.

III. THE BFS METHOD FOR ALLOYS

The BFS method for alloys[2–5] fulfills several requirements for applicability in terms of simplicity, accuracy, and range of application, as it has no limitations in its formulation on the number and type of elements present in a given alloy. Moreover, it has shown promise in describing diverse problems, particularly in the area of surface alloys[2] and high-temperature ordered intermetallics.[3–5] The method provides a simple algorithm for the calculation of the energy of formation ΔH of an arbitrary alloy (the difference between the energy of the alloy and that of its individual constituents), written as the superposition of elemental contributions ε_i of all the atoms in the alloy, where ε_i denotes the difference in energy between a given atom in the equilibrium alloy and in an equilibrium single crystal of species i:

$$\Delta H = \sum_i \varepsilon_i \tag{1}$$

For each atom, we partition the energy into two parts: a strain energy, ε_i^S, and a chemical energy, ε_i^C, contribution. By definition, the BFS strain and chemical energy contributions take into account different effects, i.e., geometry and compo-

sition, computing them as isolated effects. A coupling function, g_i, restores the relationship between the two terms by considering the asymptotic behavior of the chemical energy, where chemical effects are negligible for large separations between dissimilar atoms. A reference chemical energy, $\varepsilon_i^{C_0}$, is also included to insure a complete decoupling of structural and chemical features. Summarizing, the contribution to the energy of formation of atom i is then

$$\varepsilon_i = \varepsilon_i^S + g_i(\varepsilon_i^C - \varepsilon_i^{C_0}). \tag{2}$$

The BFS strain energy, ε_i^S, differs from the commonly defined strain energy in that the actual chemical environment is replaced by that of a monoatomic crystal. Its calculation is then straightforward, even amenable to FP methods. In this work, however, we use for its computation the equivalent crystal theory (ECT),[11] due to its ability to provide accurate and computationally economical answers to most general situations. The BFS strain energy contribution, ε_i^S, is obtained by solving the ECT perturbation equation

$$NR_1^{p_i}e^{-\alpha_i R_1} + MR_2^{p_i}e^{-(\alpha_i+1/\lambda_i)R_2} = \sum_j r_j^{p_i}e^{-[\alpha_i+S(r_j)]r_j}, \tag{3}$$

where N and M are the number of nearest-neighbors (NN) and next-nearest neighbors (NNN) at distances R_1 and R_2 (in the equivalent crystal), respectively, and where p, l, α, and λ are ECT parameters that describe element i (see Ref. 11 for definitions and details), r denotes the distance between the reference atom and its NN and NNN, and $S(r)$ describes a screening function[11] for NNN. This equation is used for the calculation of the lattice parameter a_i^S of a perfect crystal where the reference atom i has the same energy as it has in the geometrical environment of the alloy under study. Once the lattice parameter of the (strain) equivalent crystal, a_i^S, is determined, ε_i^S is computed using the UBER of Rose *et al.*,[8] which contains all the relevant information concerning a single-component system

$$\varepsilon_i^S = E_{C,i}[1 - (1 + a_i^{S*})e^{-a_i^{S*}}] \tag{4}$$

where $E_{C,i}$ is the cohesive energy of atom i and where the scaled lattice parameter $a_i^{S^*}$ is given by

$$a_i^{S*} = q\frac{(a_i^S - a_{e,i})}{l_i}, \tag{5}$$

where q is the ratio between the equilibrium Wigner-Seitz radius and the equilibrium lattice parameter, $a_{e,i}$.

The BFS chemical energy, ε_i^C, is obtained by a similar procedure. As opposed to the strain energy term, the surrounding atoms retain their chemical identity, but are forced to be in equilibrium lattice sites of an equilibrium crystal of atom i. The BFS equation for the chemical energy is given by

$$NR_1^{p_i}e^{-\alpha_i R_1} + MR_2^{p_i}e^{-(\alpha_i+1/\lambda_i)R_2} = \sum_k [N_{ik}r_1^{p_i}e^{-\alpha_{ik}r_1} + M_{ik}r_2^{p_i}e^{-(\alpha_{ik}+1/\lambda_i)r_2}], \tag{6}$$

where N_{ik} and M_{ik} are the number of NN and NNN of species k around atom i. The chemical environment surrounding atom i, reflected in the parameter Δ_{ki}, is given by

$$\alpha_{ik} = \alpha_i + \Delta_{ki} \tag{7}$$

where the BFS parameter Δ_{ki} (a perturbation on the single-element ECT parameter α_i) describes the changes of the wave function in the overlap region between atoms i and k. Once Eq. (6) is solved for the equivalent chemical lattice parameter, a_i^c, the BFS chemical energy is then

$$\varepsilon_i^C = \gamma_i E_{C,i}[1 - (1 + a_i^{C*})e^{-a_i^{C*}}] \tag{8}$$

where $\gamma_i = 1$ if $a_i^{C^*} > 0$ and $\gamma_i = -1$ if $a_i^{C^*} < 0$, and the scaled chemical lattice parameter $a_i^{C^*}$ is given by

$$a_i^{C*} = q\frac{(a_i^C - a_{e,i})}{l_i}. \tag{9}$$

Finally, as mentioned earlier, the BFS strain and chemical energy contributions are linked by a coupling function g_i, which describes the influence of the geometrical distribution of the surrounding atoms in relation to the chemical effects and is given by

$$g_i = \exp(-a_i^{S*}). \tag{10}$$

The computation of ε_i^S and ε_i^C, using ECT,[11] involves three pure element properties for atoms of species i: cohesive energy, lattice parameter, and bulk modulus. The chemical energy, ε_i^C, includes two BFS perturbative parameters (Δ_{ki} and Δ_{ik}, with i, k including all possible binary combinations of the alloy constituents). Table I lists all the parameters for the pure elements used in the different examples in this work.

TABLE I. Ground state parameters of different elements. The equilibrium lattice parameter (in angstroms), cohesive energy (in electron-volts), and scaling length (in angstroms) provide the best fit of the first-principles data for the total energy vs lattice parameter via the universal binding energy relation of Rose *et al.* (see Ref. 8).

Element	a_e (Å)	E_c (eV/atom)	l (Å)
Ni (fcc)	3.5184	5.6724	0.2996
Ni (bcc)	2.7975	5.6207	0.2904
Al (fcc)	4.0459	3.5378	0.3517
Al (bcc)	3.2379	3.4423	0.3641
Ti (fcc)	4.1103	5.8244	0.3782
Ti (bcc)	3.2561	5.7721	0.3814
Cr (fcc)	3.6184	4.9640	0.2472
Co (fcc)	3.4580	5.5637	0.2617
Fe (fcc)	3.4452	4.2700	0.2124

IV. RELATIONSHIP BETWEEN BFS AND *AB INITIO* METHODS

In this section we elaborate further on the concepts introduced in Sec. III and examine the performance of the method in the framework of FP calculations. Comparable in

simplicity but different in its formulation from other qams, the BFS method for alloys is based on a different way of interpreting the alloy formation process. Any given system, regardless of its composition and structure, is always modeled in terms of two independent virtual processes which, properly coupled, are meant to result in the final state that is being studied. One of these virtual processes relates to the structural changes in the environment of any given atom (strain energy). The other virtual process accounts for changes in the chemical environment of that same atom (chemical energy). To decouple structural and chemical effects, in the strain process all atoms surrounding a given atom are considered as being of the same atomic species as the reference atom, thus freezing compositional degrees of freedom. In the chemical process, the surrounding atoms retain their chemical identity, but are forced to occupy equilibrium lattice sites of a lattice characteristic of the reference atom. The fact that the chemical energy is a constant (for a fixed composition), can be used to our advantage and, as will be seen later, allows for an ideal integration of detailed FP calculations with the simplicity of quantum approximate methods. Both processes are based on the concept of ideal equivalent crystals. As such, the method will be equally accurate when describing bulk or surface problems, as both will be mapped onto isotropically deformed equivalent crystals, properly described by the same set of parameters. The accuracy of this aspect of the approach is supported by the fact that the transformations describing the mapping of the real systems onto equivalent crystals is substantiated by perturbation theory.[11] However, the correspondence between the virtual processes and real situations or their interpretation as components of the process of alloy formation does not necessarily guarantee that the results will be accurate or comparable to those obtained with FP methods. The two virtual processes, associated to the calculation of the strain and chemical energy, are defined independently, although it is clear that the appropriate coupling of the two processes is what ultimately determines the validity of the method. Once the choice is made to depart from a straight description of the real process and virtual processes are chosen to replace them, the freedom in the features describing each virtual process is constrained by the fact that, ultimately, the coupling between them has to be such that the final state coincides with the actual alloy or system under study. The coupling function g plays the role of linking the structural and chemical information of the system in a straightforward and computationally economical way (i.e., no additional calculations are required to determine the value of g for every single atom in the computational cell). As defined in Eq. (10), g ensures the correct asymptotic behavior of the chemical energy. If the scaled lattice parameter $a_i^{S^*}$ is understood as a measure of the structural characteristics of the alloy from the perspective of each individual atom i, then a positive value of $a_i^{S^*}$ means that the atom i finds itself in an atomic local environment that resembles an isotropically expanded version of a pure crystal of species i. As such, the chemical environment (i.e., the changes in the electron density in the vicinity of atom i due to the presence of neighbors with different chemical identities) is diminished. Conversely, if $a_i^{S^*}$ is negative, the opposite is true. The exponential form of the coupling function is chosen as the simplest form (i.e., no additional parameters are introduced in its definition) that describes the asymmetry between the two regimes: the possibility of an infinite expanded equivalent crystal is not matched by a corresponding infinite compression.

It remains to be shown that this simple way of coupling the two processes suffices to warrant results that would be comparable to those obtained from FP calculations. To this end, we concentrate on the expression for the energy of formation in terms of the individual constituents as provided by Eqs. (1) and (2):

$$\Delta H = \sum_i \varepsilon_i^S + g_i(\varepsilon_i^C - \varepsilon_i^{C_0}). \tag{11}$$

Consider a compound $(ABC\ldots Z)$. The energy of formation of such compound can be written as

$$\Delta H = E - \sum_X E_X^0, \tag{12}$$

where E is the total energy of the compound, and E_X^0 is the energy of atoms of species $X(X=A,B,C,\ldots,Z)$ at equilibrium. The total energy of the compound can also be written in terms of the equilibrium energy of each one of its components ($E_{X,j}$), computed from the minimum of the UBER (or any other equation of state at $T=0$ K), and an "alloying" term, $E_{residual}$, as follows

$$E = \sum_{X,j} E_{X,j} + E_{residual}, \tag{13}$$

where the sum runs over all atoms j of species X. Combining these two expressions, we obtain

$$\Delta H = \sum_{X,j} (E_{X,j} - E_X^0) + E_{residual}. \tag{14}$$

This last expression can now be compared to the BFS expression for the energy of formation in terms of strain and chemical components, given in Eq. (11), reformatted to single out the energy contributions from monoatomic crystals

$$\Delta H = \sum_{X,j} \varepsilon_{X,j}^S + \varepsilon_{residual}. \tag{15}$$

Thus, BFS extracts the maximum amount of information of a given compound from the single element UBERs, with $\varepsilon_{residual}$ responsible for any additional information regarding the mixing process. In BFS, this quantity is written as a linear combination of the coupling functions $g_{X,i}$ assigned to each atom j of element $X(X=A,B)$:

$$\varepsilon_{residual} = \sum_{X,j} \mu_{X,j} g_{X,j} \tag{16}$$

and the constants $\mu_{X,j}$ denote the chemical energies of atom j of species X. Finally

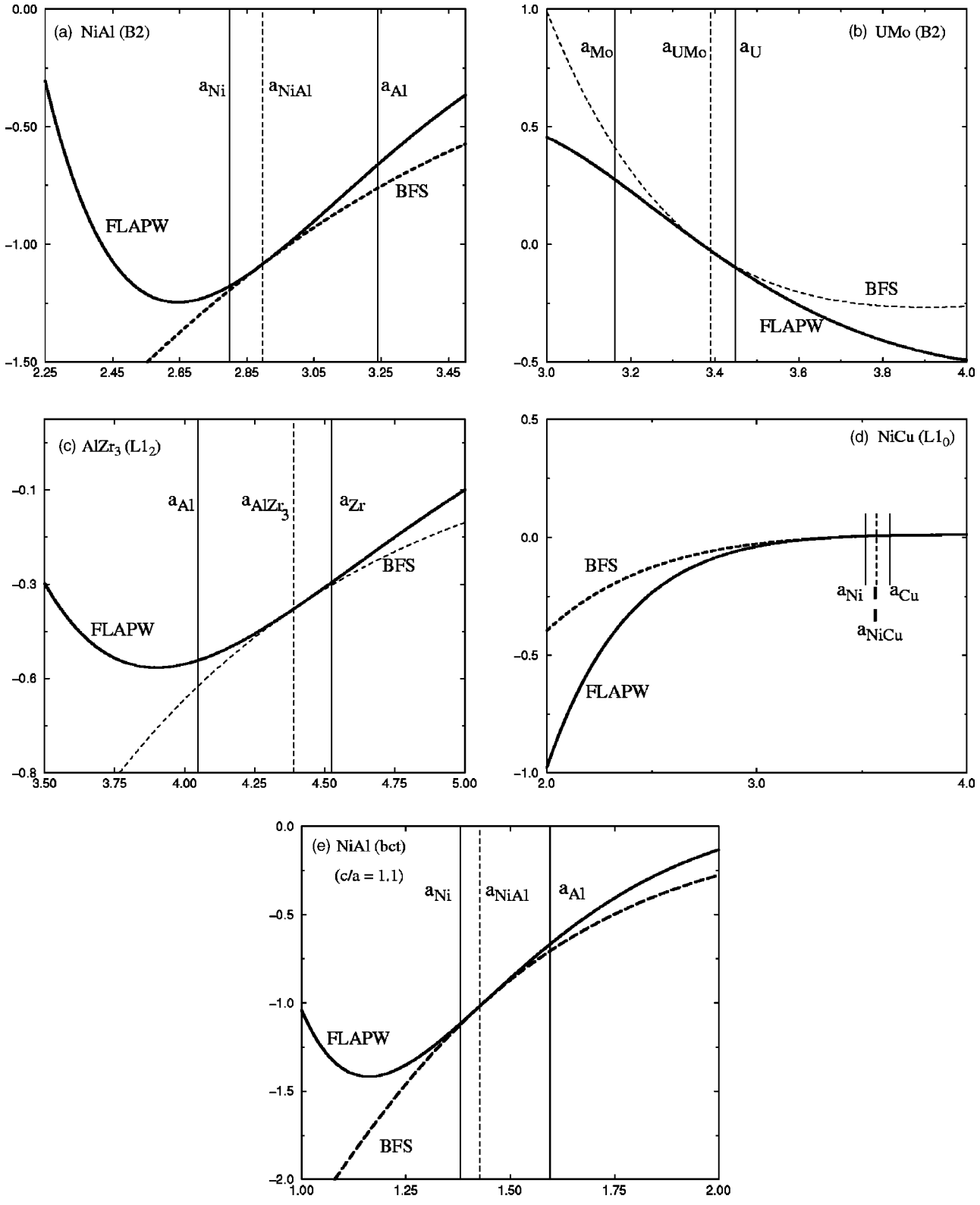

FIG. 1. Comparison of the lhs (FLAPW results, solid curves, in electron-volts per atom) and rhs (BFS results, dashed curves) of Eq. (17), as a function of lattice parameter (in angstroms), for (a) NiAl ($B2$), (b) UMo ($B2$), (c) $AlZr_3$ ($L1_2$), (d) NiCu ($L1_0$), and (e) body-centered-tetragonal NiAl ($c/a=1.1$). In this last case, the Wigner-Seitz radius is used instead of the lattice parameter. The vertical lines denote the equilibrium lattice parameters of the individual elements (in the symmetry of the alloy, dashed line) and the lattice parameter of each ordered structure (solid lines), as predicted by first-principles methods.

$$\Delta H - \sum_{X,j} (E_{X,j} - E_X^0) = \sum_{X,j} \mu_{X,j} g_{X,j}. \tag{17}$$

The left-hand side (lhs) of Eq. (17) denotes quantities that can be properly described by FP-determined UBERs, whereas the right-hand side (rhs) denotes a quantity that is exclusively computed within the context of BFS. If the method provides an accurate description of the mixing process and if the parameterization of the elements is properly included, then the validity of BFS is warranted when the identity between both terms is satisfied within the range of validity of the description of the system as provided by the UBER (i.e., in the vicinity of equilibrium). To illustrate this point, Fig. 1 displays results for a variety of binary systems. Figures 1(a) and 1(b) show the results for two ordered $B2$ (bcc) compounds, NiAl and UMo. The comparison between these two examples highlights the fact that BFS is equally accurate regardless of the type of element considered. Figures 1(c) and 1(d) refer to fcc compounds, $AlZr_3$ ($L1_2$) and NiCu ($L1_0$), respectively, indicating that the approach is equally applicable regardless of the lattice mismatch between the constituents or the type of lattice (bcc or fcc) or, as shown in Fig. 1(e) for the case of body-centered-tetragonal NiAl (with $c/a=1.1$), the specific geometry of the cell.

The agreement between FLAPW results and BFS shown in Fig. 1 is the foundation for the quality of the results found in a number of applications of the method to binary systems.[2–5] However, the examples shown in Fig. 1 represent just a few simple cases and raises the question of whether this agreement could be dependent on the complexity of the example chosen, as it relies on the ability of the FP-based parameters to carry the necessary information to warrant reasonable agreement in the equilibrium region. To further illustrate this point of additional complexity (i.e., more nonequivalent atoms, more components, etc.) and its effect on the validity of the approach, Fig. 2 shows similar results for a ternary case, an $L1_2$ Ni_2AlTi Heusler alloy. Once again, BFS results are in excellent agreement with the FP results in the equilibrium region. Recent applications to systems with up to 12 elements[12] indicate that this correspondence between FP and BFS results could be expected for any number of components.

We conclude this section noting that while Fig. 1 illustrates the ability to describe the alloy formation process by means of just a few examples for bcc or fcc systems, nothing in the formulation of the method or the derivation above imposes restrictions on the type of symmetry examined. Recent results by Légaré *et al.*[13] indicate that similar conclusions can be drawn for hcp systems. Similarly, the methodology does not impose restrictions on the number of elements in the system at hand, and no loss in accuracy should be expected for higher-order systems.

V. DETERMINATION OF GROUND STATE PROPERTIES

The simplicity of the BFS formalism allows for a straightforward analytical algorithm for the determination of ground state properties of ordered alloys. For ordered structures, Eq. (1) is substantially simplified, as it can always be reduced to

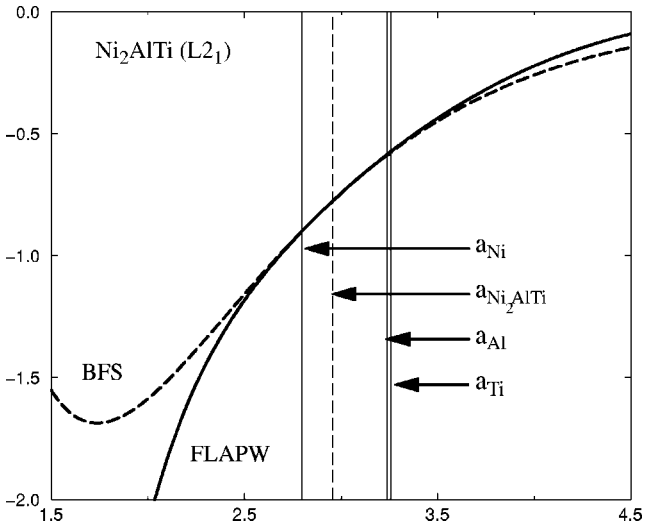

FIG. 2. Comparison of the lhs (FLAPW results, solid curves, in electron volts per atom) and rhs (BFS results, dashed curves) of Eq. (17), as a function of lattice parameter (in angstroms), for Ni_2AlTi ($L2_1$). The vertical lines denote the equilibrium lattice parameters of the individual elements (in the symmetry of the alloy, dashed line) and the lattice parameter of each ordered structure (solid lines), as predicted by first-principles methods.

the contributions of just the M nonequivalent atoms, ε_i, each with multiplicity m_i:

$$\Delta H = \sum_{i=1}^{M} m_i \varepsilon_i = \sum_{i=1}^{M} m_i (\varepsilon_i^S + g \varepsilon_i^C), \tag{18}$$

where ε^S is the strain energy, ε^C is the chemical energy, and g is the coupling function for each of the M nonequivalent atoms.

If the value of ΔH is known for M arbitrary values of the lattice parameter a, then the chemical energies can be easily obtained by simply solving a linear system of equations based on the values $\Delta H(a_k)=\Delta H_k$ ($k=1,\ldots M$). Once these energies are known, the equilibrium properties of the alloy can be trivially obtained by minimization of ΔH. Most simple binary structures have just one nonequivalent atom of each kind. These are, for example, the bcc-based $B2$ and fcc $L1_0$ structures. $D0_{22}$, $D0_3$, and $L6_0$ AB_3 binary ordered structures require one A and two different B atoms. Also, ternary ordered structures, as $L2_1$ A_2BC, would require a minimum of three nonequivalent atoms. Although the formalism can be presented for an arbitrary number M of nonequivalent atoms, we will illustrate it, for the sake of brevity, with simple $B2$ or $L1_0$ structures. It should be noted, however, that some restrictions or simplifications were imposed in these calculations due only to the fact that they do not address the objective of this work (i.e., to introduce the concepts), and not because it is outside the scope of the methodology.

For these structures, the BFS energy of formation is simply

$$\Delta H = \tfrac{1}{2}(\varepsilon_A^S + g_A \varepsilon_A^C + \varepsilon_B^S g_B + \varepsilon_B^C), \tag{19}$$

where ε_X^S and ε_X^C denote the strain and chemical energy,

respectively, of atom X. While the strain energy contributions(and the corresponding coupling functions g_X) are volume dependent, the chemical energies are not, and can be easily computed if just two FP-computed energies of formation ΔH_1 and ΔH_2, are known. In principle, these two energies could correspond to any two arbitrary values a_1 and a_2 of the lattice parameter, which we will represent by their corresponding Wigner-Seitz radii, r_1 and r_2. Using Eq. (19), it is straightforward to compute the chemical energies from ΔH_1 and ΔH_2:

$$\varepsilon_A^C = \frac{g_B^{(2)}[2\Delta H_1 - \varepsilon_A^S(r_1) - \varepsilon_B^S(r_1)] - g_B^{(1)}[2\Delta H_2 - \varepsilon_A^S(r_2) - \varepsilon_B^S(r_2)]}{[g_A^{(1)} g_B^{(2)} - g_A^{(2)} g_B^{(1)}]}, \tag{20}$$

where $g_i^{(k)} = g_i(r_k)$. A similar expression results for ε_B^C, exchanging A for B. If, as shown in Sec. IV, the method is successful in describing the process of alloy formation, then the computed values of ε_A^C and ε_B^C can be used for the determination of the equilibrium lattice parameter a_0 of the alloy, by solving

$$\left.\frac{d(\Delta H)}{dr}\right|_{a_0} = 0. \tag{21}$$

Once a_0 is known, the energy of formation of the equilibrium ordered alloy, ΔH_0, is obtained with Eq. (19). The results should be equivalent to the values obtained from FP calculations.

The procedure can be further simplified if some reasonable expression denoting isotropic expansions or compressions of each single crystal is used for $\varepsilon_A^S(a)$ and $\varepsilon_B^S(a)$. It should be noted, however, that the following results do not depend on the functional form used. A natural and sufficiently accurate expression is given by the universal binding energy relationship

$$E(r) = -E_C(1 + a^*)e^{-a^*}, \tag{22}$$

where

$$a^* = \frac{r - r_e}{l}, \tag{23}$$

and E_C and r_e represent the cohesive energy and the equilibrium Wigner-Seitz radius of the pure element, respectively, and l is related to the bulk modulus by

$$l = \sqrt{\frac{E_C}{12\pi B_0 r_e}}. \tag{24}$$

After using the UBER (or any other alternative expression), Eq. (21) simply reads

$$\frac{g_A}{l_A}(E_C^A a_A^{S^*} - \varepsilon_A^C) + \frac{g_B}{l_B}(E_C^B a_B^{S^*} - \varepsilon_B^C) = 0. \tag{25}$$

Moreover, once ΔH_0 and a_0 are known, the bulk modulus B_0 can be computed from these expressions (assuming that the alloy can also be described by an UBER), by means of the scaling length l_0 [see Eq. (24)]:

$$l_0 = \sqrt{\frac{E_C^A + E_C^B - 2\Delta H_0}{\frac{g_A}{l_A^2}[E_C^A(1 - a_A^{S^*}) + \varepsilon_A^C] + \frac{g_B}{l_B^2}[E_C^B(1 - a_B^{S^*}] + \varepsilon_B^C]}}. \tag{26}$$

Generally, the path followed when using FP calculations to produce input parameters to fit alloy properties in qams consists of determining the full energy versus lattice parameter curve, and then fit the results to appropriate functional forms to extract the equilibrium alloy properties. The present algorithm, instead, simplifies this procedure by combining limited FP input with BFS to provide ΔH_0, a_0, and l_0, in a straightforward fashion, thus optimizing the transfer of information.

It is important to stress that the methodology is general enough to be applicable to multicomponent systems, complex ordered structures, etc., where it is imperative to simplify the computational work maximizing, at the same time, the amount and quality of information that can be obtained for the system at hand.

The accuracy and relevance of the procedure is demonstrated in the following examples. Using FLAPW input (fitted to a UBER) to determine the pure element parameters (a, E_c, l), listed in Table I, Table II shows typical results for the values of $(a_0, \Delta H_0, l_0)$ obtained both from a direct fit of FP results and with the algorithm outlined in Sec. V, using the equilibrium values of the lattice parameter of elements A and B as the two reference points a_1 and a_2. Table III supplements these results with a comparison between theoretical[14–20] and experimental[21–32] data for some of these systems.

As a final point, and in order to maximize the quality of the information carried by the relevant parameters, it is important to mention that even small instabilities in FP calculations (for example, uncertainties in the values of ΔH_1 or ΔH_2 in Eq. (20)) could have a deleterious effect on the accuracy of the BFS parameters Δ that can be extracted from the computed values of the chemical energies [Eq. (20)], and therefore limit their ability to properly describe the system under study. As an example of the reliance of this algorithm on the accuracy of the FP input, Fig. 3 shows typical results for NiAl in the $B2$ and $L1_0$ structures, highlighting the role of the chemical energies in the determination of the binding energy curve for each alloy. As described earlier, the algo-

TABLE II. Comparison between the equilibrium lattice parameter (in angstroms), energy of formation (electron-volts per atom), and scaling length (in angstroms) obtained from fitting FLAPW data with the universal binding energy curve of Rose *et al.* (see Ref. 8), and the predictions of the same parameters obtained from Eqs. (25) and (26) using the FLAPW+BFS approach introduced in Sec. V. The two reference points (a_1 and a_2) used in the FLAPW+BFS approach correspond to the equilibrium values of the lattice parameter of the single elements.

	FLAPW (This work)			Limited FLAPW input+BFS		
Alloy	a_0 (Å)	ΔH_0 (eV/atom)	l_0 (Å)	a_0 (Å)	ΔH_0 (eV/atom)	l_0 (Å)
NiAl ($B2$)	2.8951	−0.7598	0.3131	2.8958	−0.7582	0.3230
NiAl ($L1_0$)	3.6676	−0.5431	0.3176	3.6658	−0.5427	0.3244
Ni_3Al ($L1_2$)	3.5652	−0.4732	0.3065	3.5651	−0.4731	0.3016
NiTi ($B2$)	3.0148	−0.4728	0.3318	3.0146	−0.4706	0.3421
AlTi ($L1_0$)	4.0224	−0.4367	0.3534	4.0213	−0.4366	0.3678
AlTi ($B2$)	3.1880	−0.3677	0.3490	3.1820	−0.3682	0.3741
CrFe ($L1_0$)	3.5250	−0.1339	0.2569	3.5255	−0.1354	0.2550
NiCr ($L1_0$)	3.5469	−0.1545	0.2669	3.5457	−0.1545	0.2694
AlCo ($B2$)	2.8522	−0.8632	0.2984	2.8518	−0.8631	0.3067
AlCo ($L1_0$)	3.6382	−0.4451	0.2986	3.6371	−0.4450	0.3028
CoCr ($L1_0$)	3.5156	−0.2649	0.2546	3.5156	−0.2652	0.2536
AlFe ($B2$)	2.8693	−0.5866	0.2983	2.8691	−0.5865	0.3053
AlFe ($L1_0$)	3.6547	−0.1639	0.2977	3.6510	−0.1651	0.3016

TABLE III. A sample of theoretical (Refs. 14–20) and experimental (Refs. 21–32) results for the equilibrium lattice parameter a_0 (in angstroms) and energy of formation per atom ΔH_0 (in electron-volts per atom) for some of the binary alloys listed in Table II. The asterisk indicates the observed structure.

	a_0 (Å)			ΔH_0 (eV/atom)		
Alloy	FP This work	Exp. Ref. 21	Theor. Ref. 14	FP This work	Exp.	Theory
NiAl ($B2$)*	2.8951	2.8864	2.8332	−0.7598	−0.60[a], −0.74[b], −0.69[c] −0.68[d], −0.68[d] −0.70[e], −0.64[f]	−0.70[l] −0.78[m], −0.83[n], −0.72[n] −0.65[o], −0.74[p]
NiAl ($L1_0$)	3.6676		3.5698	−0.5431		−0.54[r], −0.58[m]
Ni_3Al ($L1_2$)*	3.5652	3.567	3.4746	−0.4732	−0.40[c], −0.43[g], −0.42[h], −0.49[e]	−0.46[r], −0.50[m]
NiTi ($B2$)*	3.0148	3.015	2.9226	−0.4728	−0.35[i], [j]	−0.35[l], −0.42[n], −0.47[n], −0.45[q]
AlTi ($L1_0$)*	4.022 ($c/a=1$)	4.005 ($c/a=1.02$)	3.9715	−0.4367	−0.39[b], −0.38[b], −0.37[c], −0.38[k]	−0.41[l], −0.44[s]
AlTi ($B2$)	3.1880		3.1528	−0.3677		−0.26[l]
AlFe ($B2$)*	2.8693 (nonmagnetic)	2.909	2.8205	−0.5866	−0.25[i], −0.26[k], −0.28[c]	−0.42[l]
AlFe ($L1_0$)	3.6547 (nonmagnetic)		3.5534	−0.1639		−0.17[l]

[a]See Ref. 22.
[b]See Ref. 23.
[c]See Ref. 24.
[d]See Ref. 25.
[e]See Ref. 26.
[f]See Ref. 27.
[g]See Ref. 28.
[h]See Ref. 29.
[i]See Ref. 30.
[j]See Ref. 31.
[k]See Ref. 32.
[l]See Ref. 14.
[m]See Ref. 15.
[n]See Ref. 16.
[o]See Ref. 17.
[p]See Ref. 18.
[q]See Ref. 19.
[r]See Ref. 13.
[s]See Ref. 20.

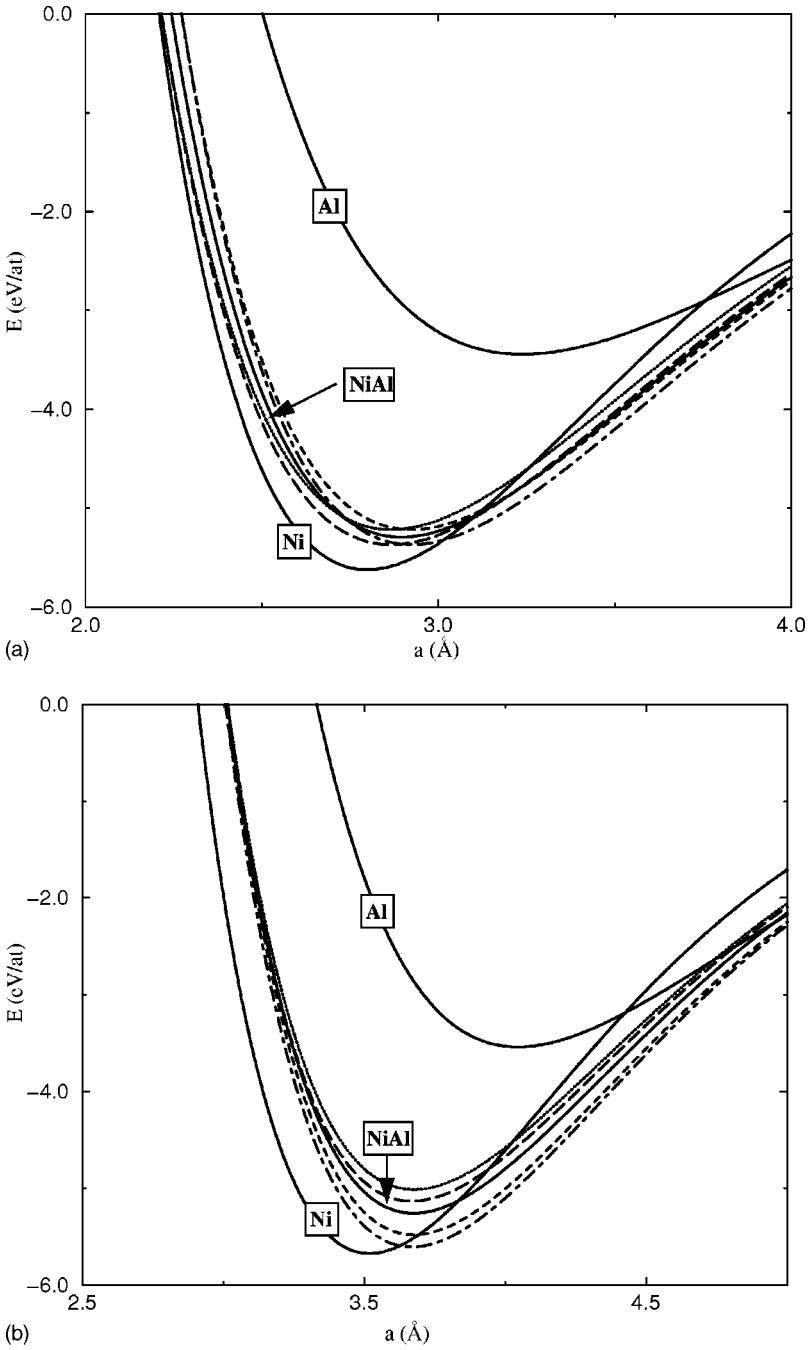

FIG. 3. Binding energy curves for *AB* alloys. The solid curves describe the pure elements (Ni, Al) and the binary alloys NiAl in different structures: (a) $B2$ and (b) $L1_0$. The other curves denote the predictions based on variations of the equilibrium lattice parameter a_0 and the energy of formation (ΔH_0) of $(-1\%, -10\%)$ (dots), $(+1\%, -10\%)$ (dashed line), $(-1\%, +10\%)$ (long dashed line) and $(+1\%, +10\%)$ (dot-dashed line).

rithm relies on the determination of the chemical energies of each nonequivalent atom which, via Eq. (19), define the binding energy curve for the alloy. We note that in the same way that the chemical energies can be determined from Eq. (20), they can also be obtained from $(a_0, \Delta H_0)$ (as long as Eq. (21) is satisfied)

$$\varepsilon_A^C = \frac{2(\Delta H_0 - \Delta H_S)}{g_A^{(0)}\left(1 - \frac{l_B}{l_A}\right)} + E_C^A a_A^{s^*}(a_0), \tag{27}$$

where

$$g_A^{(0)} = e^{-a_A^{s^*}(a_0)} \tag{28}$$

and

$$\Delta H_S = \tfrac{1}{2}[E_C^A(1 - g_A^{(0)}) + E_C^B(1 - g_B^{(0)})], \tag{29}$$

(and a similar expression for ε_B^C). In Fig. 3, besides plotting the binding energy curve for each pure element, we include the UBER for the alloy when the FP values of $(a_0, \Delta H_0)$ are used. We also include alternative results for this same curve, also obtained from Eq. (3), but where the FP input $(a_0, \Delta H_0)$ has been increased or decreased by 1% (for the lattice parameter) and 10% (for the energy of formation). While little variation is seen for NiAl $B2$, substantial dispersion of the

predicted values occurs in the NiAl $L1_0$ structure, underscoring the sensibility of the FLAPW+BFS algorithm against small variations in the FP input used. In light of this feature, it is not surprising that the stability of the BFS predictions are directly linked to the quality and precision of the input used. Accurate and precise theoretical or experimental input will result in correspondingly accurate BFS predictions, and conversely, unstable input would translate into dispersion of the results (as seen in Fig. 3(b)).

VI. CONCLUSIONS

High expectations have been imposed on the range of applicability of quantum approximate methods, their computational efficiency, their ease of implementation, and the type of output that they provide. The particular partitioning of the energy of formation of an alloy in the framework of the BFS method allows for the determination of the equilibrium alloy properties from FP input of the pure elements and limited data points for the alloy, obtained also from such calculations. In this paper we show that it is possible to model the process of alloy formation with a minimum number of parameters in the vicinity of equilibrium, as shown in Figs. 1 and 2. The lack of limitations on the method regarding the number of elements present in an alloy enables the study of multicomponent systems with the same simplicity observed in the example earlier for binary systems. In this sense, and due to the potential important applications in studying systems of practical use, the algorithm in Sec. IV serves the purpose of simplifying the modeling effort to tractable levels.

ACKNOWLEDGMENTS

Fruitful discussions with N. Bozzolo are gratefully acknowledged. We would like to thank J. Morse for his assistance in preparing this manuscript. This work was sponsored by the Alternative Energy Foundation Technologies Subproject of the Low Emissions Alternative Power Project at the NASA Glenn Research Center, Cleveland, Ohio.

[1] S. Cottenier, Phys. Mag. **26**, 3 (2004).
[2] G. Bozzolo and J. E. Garcés, in *The Chemical Physics of Solid Surfaces*, edited by D. P. Woodruff (Elsevier, New York, 2002), p. 30.
[3] G. Bozzolo, H. O. Mosca, A. W. Wilson, R. D. Noebe, and J. E. Garcés, Metall. Trans. B **33**, 265 (2002).
[4] A. W. Wilson, G. Bozzolo, R. D. Noebe, and J. Howe, Acta Mater. **50**, 2787 (2002).
[5] P. Gargano, H. Mosca, and G. Bozzolo, Scr. Mater. **48**, 695 (2003).
[6] O. K. Andersen, Phys. Rev. B **12**, 3060 (1965).
[7] P. Blaha, K. Schwartz, and J. Luitz, WIEN97, Vienna University of Technology. Improved and updated Unix version of the copyrighted WIEN code; P. Blaha, P. Schwartz, P. Sorantin, and S. B. Trickey, Comput. Phys. Commun. **59**, 399 (1990).
[8] J. H. Rose, J. R. Smith, and J. Ferrante, Phys. Rev. B **28**, 1835 (1983).
[9] J. P. Perdew, K. Burke, and M. Ernzerhof, Phys. Rev. Lett. **77**, 3865 (1996).
[10] D. J. Singh, Phys. Rev. B **43**, 6388 (1991).
[11] J. Smith, T. Perry, A. Banerjea, J. Ferrante, and G. Bozzolo, Phys. Rev. B **44**, 6444 (1991).
[12] P. Abel and G. Bozzolo, Scr. Mater. **46**, 557 (2002).
[13] P. Légaré, G. F. Cabeza, and N. J. Castellani, Surf. Sci. **441**, 461 (1999).
[14] R. E. Watson and M. Weinert, Phys. Rev. B **58**, 5981 (1998).
[15] A. Pasturel, C. Colinet, A. T. Paxton, and M. van Schilfgaarde, J. Phys.: Condens. Matter **4**, 945 (1992); Z. W. Lu, S. H. Wei, A. Zunger, S. Frota-Pessoa, and L. G. Ferreira, Phys. Rev. B **44**, 512 (1991).
[16] B. P. Burton, J. E. Osburn, and A. Pasturel, Phys. Rev. B **45**, 7677 (1992).
[17] P. A. Schultz and J. W. Davenport, Scr. Metall. Mater. **27**, 629 (1992).
[18] W. Lin and A. J. Freeman, Phys. Rev. B **45**, 61 (1992).
[19] C. Colinet and A. Pasturel, Physica B **192**, 238 (1993).
[20] M. Asta, D. de Fontaine, M. van Schilfgaarde, M. Sluiter, and M. Methfessel, Phys. Rev. B **46**, 5055 (1992).
[21] W. B. Pearson, *Handbook of Lattice Spacings and Structure of Metals* (Pergamon Press, Oxford, 1967).
[22] O. J. Kleppa, J. Phase Equilib. **15**, 240 (1994).
[23] F. R. de Boer, R. Boom, W. C. M. Mattens, A. R. Miedema, and A. K. Niessen, *Cohesion in Metals* (North-Holland, Amsterdam, 1988).
[24] P. D. Desai, J. Phys. Chem. Ref. Data **16**, 109 (1987).
[25] K. Rzyman, Z. Moser, R. E. Watson, and M. Weinert, J. Phase Equilib. **19**, 106 (1998).
[26] V. M. Es'kov, V. V. Samokhval, and A. A. Vecher, Russ. Metall. **2**, 118 (1974).
[27] J. Wang and H. J. Engell, Steel Res. **63**, 320 (1992).
[28] K. Rzyman, Z. Moser, R. Watson, and M. Weinert, J. Phase Equilib. **17**, 173 (1996).
[29] S. Kek, K. Rzyman, and F. Sommer, An. Fis., Ser. B **86**, 31 (1990).
[30] R. Hultgren, P. D. Desai, D. T. Hawkins, M. Gleiser, and K. K. Kelley, *Selected Values of Thermodynamic Properties of Binary Alloys* (American Society for Metals, Metals Park, OH, 1973).
[31] J. C. Gachon and J. Hertz, CALPHAD: Comput. Coupling Phase Diagrams Thermochem. **7**, 1 (1983).
[32] *Smithells Metals Reference Book*, edited by E. A. Brandes and G. B. Brook (Butterworths, Oxford, 1992).